

# Detection of Secondary Amides in HCN Polymers by Dipolar Rotational Spin-Echo $^{15}\text{N}$ NMR

Joel R. Garbow and Jacob Schaefer\*†

Physical Sciences Center, Monsanto Company, St. Louis, Missouri 63167

Robert Ludicky and C. N. Matthews

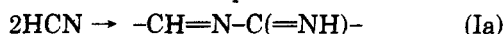
Department of Chemistry, University of Illinois at Chicago, Chicago, Illinois 60680.

Received June 20, 1986

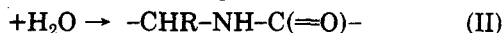
**ABSTRACT:** The solids formed by base-catalyzed polymerization of HCN or by electrical discharge through an atmosphere of methane and ammonia have been examined by cross-polarization magic-angle spinning dipolar rotational spin-echo  $^{15}\text{N}$  NMR. This experiment measures nitrogen-proton dipolar coupling and so can be used to count the average number of protons attached to a nitrogen whose NMR resonance is resolved. On the basis of such measurements, we conclude that the majority of the amidine or amide nitrogens in the base-catalyzed HCN polymers examined are secondary and hence peptide-like. This is not proof for the direct formation of heteropolypeptides from HCN, however, since none of the amidine or amide nitrogens observed are bonded to aliphatic carbons, as established by double cross-polarization  $^{13}\text{C}$  and  $^{15}\text{N}$  NMR. The anhydrous solids formed by the electrical discharge have aliphatic carbons but little or no amidine functionality, and so they too are unlikely precursors for the direct formation of heteropolypeptides.

## Introduction

Matthews et al.<sup>1-4</sup> have proposed that the original heteropolypeptides on primitive Earth may have formed spontaneously from HCN and water without the prior formation of  $\alpha$ -amino acids. This mechanism sidesteps the problems of more conventional schemes that postulate the action of various condensing agents or catalysts<sup>5</sup> to polymerize  $\alpha$ -amino acids. According to the Matthews proposal for base-catalyzed polymerization of HCN, the following series of reactions takes place:<sup>1</sup>



where R' represents any side chain that may result from the further reactions of HCN and the -CN side chain. Hydrolysis results in the final product



where R represents the result of hydrolyzing R'. In this scheme, secondary-amide, peptide-like bonds are formed.<sup>6</sup> Other plausible reaction schemes for HCN polymerization produce primary but not secondary amides. This proposal has been challenged<sup>7</sup> on the grounds that the presence of peptide bonds in HCN polymers has never been demonstrated unambiguously.

We have used double cross-polarization magic-angle spinning<sup>8,9</sup> (DCPMAS)  $^{15}\text{N}$  NMR to examine the polymer formed from  $\text{H}^{13}\text{CN}$  and  $\text{HC}^{15}\text{N}$  for the presence of secondary amides involved in  $^{13}\text{C}$ - $^{15}\text{N}$  bonds.<sup>6,10</sup> Low concentrations of such bonds have been detected. A limitation on the accuracy of this determination arises from the possibility that tautomeric isotopic exchanges generate double-labeled primary-amide bonds, which also report in the DCP experiment.<sup>10</sup>

In this paper, we use dipolar rotational spin-echo  $^{15}\text{N}$  NMR<sup>11</sup> to measure directly the average number of protons attached to the amide nitrogens, which are candidates for peptide-like bonds. The nitrogen chemical-shift region selected restricts the structures examined to amidines and amides, and the  $^1\text{H}$ - $^{15}\text{N}$  dipolar coupling identifies the amidine or amide as primary or secondary.

## Experiments

**Magic-Angle Spinning NMR.**  $^{15}\text{N}$  NMR spectra were obtained at 20.3 MHz and  $^{13}\text{C}$  NMR spectra at 50.3 MHz using matched spin-lock cross-polarization transfers with 2-ms contacts and  $H_1(\text{C or N}) = 35$  kHz. The dried samples were contained in a cylindrical double-bearing rotor spinning at 3.2 kHz. Residual spinning sidebands in the spectra were suppressed by pulse techniques.<sup>12</sup> Technical details of the spinning and cross-polarization procedures are reported elsewhere.<sup>13</sup>

Double cross-polarization  $^{15}\text{N}$  NMR spectra were obtained by using matched spin-lock transfers first from  $^1\text{H}$  to  $^{15}\text{N}$  and then from  $^{15}\text{N}$  to  $^{13}\text{C}$ .<sup>10</sup> If the  $^{13}\text{C}$  radiofrequency field is on-resonance and its amplitude satisfies the magic-angle spinning carbon-nitrogen Hartmann-Hahn condition,<sup>9</sup> a spin-lock transfer from  $^{15}\text{N}$  to  $^{13}\text{C}$  drains polarization from  $^{15}\text{N}$ . The direct difference between single and double cross-polarization experiments then results in the accumulation of a DCPMAS difference  $^{15}\text{N}$  signal arising exclusively from those nitrogens directly bonded to  $^{13}\text{C}$ . The corresponding  $^{13}\text{C}$  DCPMAS spectra were obtained by first transferring polarization from  $^1\text{H}$  to  $^{13}\text{C}$  and then from  $^{13}\text{C}$  to  $^{15}\text{N}$ . Both double cross-polarization experiments are performed by difference to remove any dependence on rotating-frame relaxation times.

**Dipolar Modulation.** Dipolar rotational spin-echo  $^{15}\text{N}$  NMR is a two-dimensional experiment in which, during the additional time dimension, the nitrogen magnetization generated by cross polarization is allowed to evolve under the influence of N-H coupling while H-H coupling is suppressed by  $^1\text{H}$  multiple-pulse irradiation. For nitrogens whose resonances are resolved, or partially resolved, in the chemical-shift dimension, a Fourier transform of intensity vs. evolution time yields a dipolar spectrum consisting of a  $^{15}\text{N}$ - $^1\text{H}$  Pake doublet, scaled by the multiple-pulse decoupling and broken up into sidebands by the magic-angle spinning. This method has been discussed before<sup>14-18</sup> and illustrated by applications to the characterization of motion in solid glassy polymers.<sup>19,20</sup> In the latter applications, C-H dipolar coupling was observed, but the analytical techniques remain the same as used for the characterization of N-H coupling. Semi-windowless MREV-8<sup>21-23</sup> homonuclear multiple-pulse decoupling was used for the experiments described here with a 16.8- $\mu\text{s}$  half-cycle period. Dipolar echo refocusing after two rotor periods was typically 80%.

**Nitrogen Dipolar Tensors.** N-H dipolar-tensor simulations were performed by using the methods developed by Herzfeld and Berger.<sup>19,24</sup> The N-H bond length was fixed at 1.01 Å.<sup>25</sup> Simulated  $^{15}\text{NH}_2$  dipolar sideband patterns were calculated as the superposition of patterns for proton spins parallel and antiparallel, respectively. An H-N-H bond angle of 120° was assumed.<sup>25</sup>

The widths of experimental NH and  $\text{NH}_2$  dipolar patterns are reduced by the ultrahigh-frequency motions common to all solids

\* Present address: Department of Chemistry, Washington University, St. Louis, MO 63130.

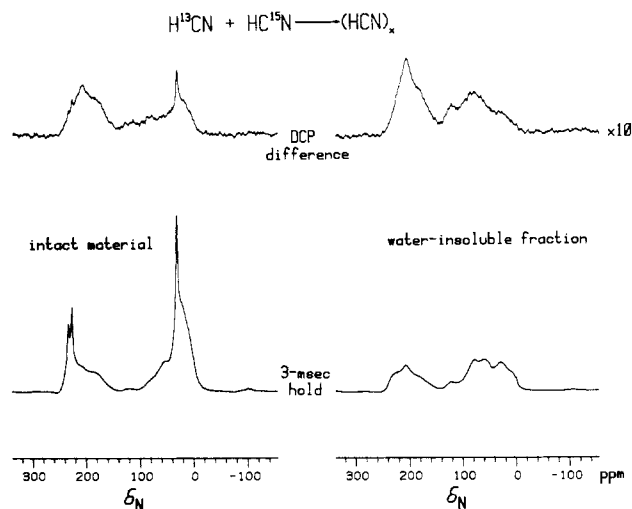


**Figure 1.** 20.3-MHz CPMAS  $^{15}\text{N}$  NMR spectra of the dried reaction products of a 1:1 mixture of  $\text{H}^{13}\text{CN}$  and  $\text{HC}^{15}\text{N}$ . The spectrum of the total solids before hydrolysis, using a 3-ms  $^{15}\text{N}$  spin-lock delay, is shown at the bottom left, and the corresponding double cross-polarization difference spectrum at the upper left of the figure. Analogous  $^{15}\text{N}$  NMR spectra of the water-insoluble fraction (which contains 82% of the total nitrogen of the intact solids) after a 30-day hydrolysis are shown at the right of the figure. The vertical scales have been adjusted so that the area of the spectrum of the insoluble fraction represents 82% of the area of the spectrum of the intact solids. The horizontal scale is in parts per million from external ammonium sulfate.

at room temperature.<sup>11,26</sup> We account for this reduction by the use of an "effective" multiple-pulse scaling factor, which is about 20% less than the theoretical scaling factor. The calculated static dipolar coupling for crystalline solids is therefore reduced by 20%, and the observed dipolar sideband patterns can then be interpreted in terms of the same C-H and N-H bond lengths established by neutron diffraction.<sup>25</sup> The theoretical semiwindowless MREV-8 scale factor is 0.54 and the effective scale factor used for the calculations reported here was 0.42.

**Polymerization.** The protocol for the HCN polymerization has been described earlier.<sup>6,10</sup> The product of this polymerization was examined by CPMAS and DCPMAS  $^{15}\text{N}$  and  $^{13}\text{C}$  NMR both before and after exposure to oxygen-free water for 30 days at room temperature. In separate experiments, the initial pH of the water was adjusted with either NaOH or HCl and NaCN to values of 3, 8.7, and 10. These conditions result in final pHs of 7.2, 9.5, and 10.6, respectively. Elemental analysis of the starting anhydrous material was typically 41% C and 47% N, and of the insoluble fraction of the water-exposed material, 35% C, 38% N, and 12% O.

Polymeric material was also produced by a version of the Miller-Urey spark experiment.<sup>5</sup> This experiment was carried out at room temperature in a 5-L flask, evacuated beforehand and then charged with  $\text{NH}_3$  (480 mmHg),  $^{15}\text{NH}_3$  (120 mmHg), and methane (600 mmHg). A Tesla coil connected to platinum electrodes provided a spark source operated for 7 days. The total product was washed with methanol. Evaporation and drying gave a dark brown solid which was examined intact by CPMAS  $^{13}\text{C}$  NMR and dipolar rotational spin-echo  $^{15}\text{N}$  NMR.

**Model Compounds.** *N*-*tert*-Butylacetamide and *N*-*tert*-butylacetamide were prepared by the method described by Fuks.<sup>27</sup> Ethyl acetamidocyanacetate was purchased from Aldrich. These compounds were examined by  $^{15}\text{N}$  and  $^{13}\text{C}$  NMR to establish typical chemical shifts for amidine-, amide-, and nitrile-substituted aliphatic carbons, respectively.  $^{15}\text{N}$  dipolar sideband patterns were obtained from experiments performed on [ul- $^{15}\text{N}$ ]allantoin and [amide- $^{15}\text{N}$ ]asparagine (Merck Stable Isotopes).

## Results

**CPMAS and DCPMAS  $^{15}\text{N}$  and  $^{13}\text{C}$  NMR.** Double cross-polarization  $^{15}\text{N}$  NMR spectra of the reaction products of an equimolar mixture of  $\text{H}^{13}\text{CN}$  +  $\text{HC}^{15}\text{N}$  (99% isotopic enrichment of both carbon and nitrogen) are

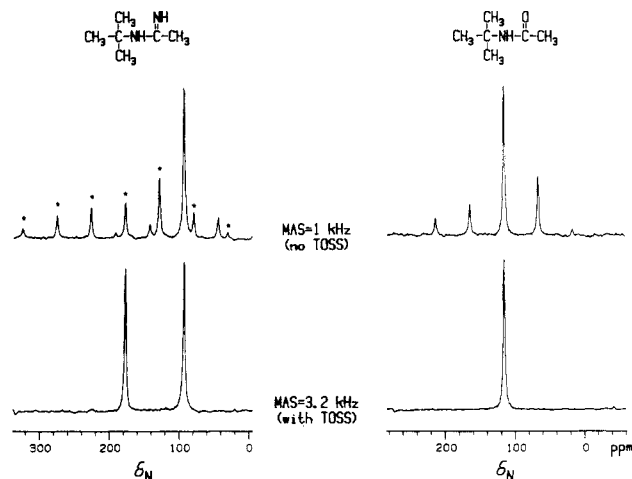


**Figure 2.** 20.3-MHz CPMAS  $^{15}\text{N}$  NMR spectra of natural-abundance model compounds containing amidine (left) and amide (right)  $\text{sp}^3$  nitrogens. Both types of nitrogens have isotropic chemical shifts near 100 ppm. The  $>\text{C}=\text{NH}$  nitrogen has a large chemical shift anisotropy, as revealed by slow spinning without total suppression of sidebands (starred peaks, top left).

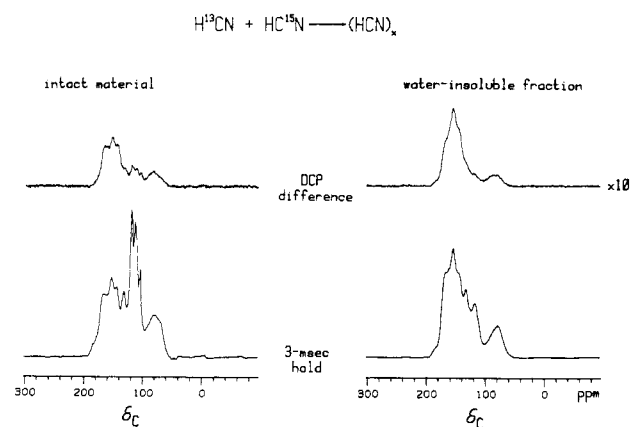


**Figure 3.** 50.3-MHz CPMAS (bottom) and DCPMAS (top)  $^{13}\text{C}$  NMR spectra of the solids described in the caption to Figure 1. The scale is in parts per million from external tetramethylsilane.

shown in Figure 1. Nitrogen appears in a wide distribution of functionalities. Before hydrolysis,  $^{15}\text{N}$  label appears in amines (40 ppm), olefinic and aromatic nitrogen (160–220 ppm), and nitrile nitrogen (240 ppm; Figure 1, left). Protonated  $=\text{NH}$  nitrogens are probably also present because of the significant intensity near 200 ppm observed following a 0.1-ms short-contact matched spin-lock transfer (spectrum not shown). After exposure to water under mild conditions, all sharp  $^{15}\text{N}$  resonances (which include signals from diaminomaleonitrile) have disappeared from the spectrum of the insoluble fraction (Figure 1, right). In addition, the shape of the broad  $^{15}\text{N}$  resonance has changed appreciably, with, for example, sizeable intensity now appearing between 90–110 ppm, the region associated with amide and amidine  $\text{sp}^3$  nitrogens. The latter assignment is based on amide and amidine model compounds<sup>28</sup> like those shown in Figure 2. There is a substantial DCP difference signal near 90 ppm for the polymer exposed to water (Figure 1, top right), but not for the anhydrous polymer (Figure 1, top left). These results are similar to those reported earlier for polymerizations of smaller amounts of labeled HCN.<sup>10</sup>

Double cross-polarization  $^{13}\text{C}$  NMR spectra of the  $\text{H}^{13}\text{CN}$  +  $\text{HC}^{15}\text{N}$  polymer are shown in Figure 3 (left). Carbon functionality is not as diverse as that observed for nitrogen. There are no aliphatic-carbon peaks between 40

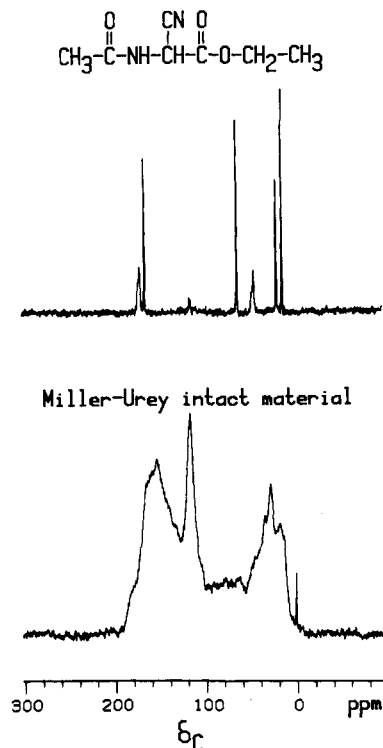


**Figure 4.** 50.3-MHz CPMAS  $^{13}\text{C}$  NMR spectra of ethyl acetamidocyanoacetate (top) and the anhydrous solids obtained from electrical discharge through an atmosphere of methane and ammonia (bottom). The resonances from carbons directly coupled to  $^{14}\text{N}$  at 45, 120, and 180 ppm are broadened by residual dipolar coupling.

and 60 ppm, which means no  $>\text{C}-\text{CN}$  groups like that, for example, of ethyl acetamidocyanoacetate. The cyano-

substituted aliphatic carbon of this model compound has an isotropic chemical shift of 45 ppm (Figure 4, top). In addition, there are no aliphatic-carbon peaks in the spectrum of the water-insoluble fraction of the water-treated HCN polymer (Figure 3, right). This is in contrast to the spectrum of the intact solids from the Miller-Urey spark experiment, which has 25% of its intensity between 20 and 40 ppm (Figure 4, bottom).

We attribute the resonance near 75 ppm in the  $^{13}\text{C}$  NMR spectrum of the HCN polymer (Figure 3, bottom left) to  $\text{sp}^3$  carbon bonded to  $^{15}\text{N}$  amines.<sup>28</sup> The sharp lines near 110 ppm (and residual spinning sidebands near 20 ppm) are due to the olefinic carbons of diaminomaleonitrile, and these disappear on exposure to water. The remaining carbon resonances are due to nitrile or  $>\text{C}=\text{NH}$  functionalities. All the carbon peaks in spectra from intact HCN materials before prolonged exposure to water, and from the water-insoluble fractions after exposure to water, have DCP signals. This means there was no formation of non-nitrogenated hydrocarbon groups. Both  $^{13}\text{C}$  and  $^{15}\text{N}$  DCPMAS spectra of the latter were insensitive to the pH conditions of water exposure (see Experiments).

**Dipolar Rotational Spin-Echo  $^{15}\text{N}$  NMR.** The CPMAS  $^{15}\text{N}$  NMR spectrum of the intact solids from the Miller-Urey spark experiment (Figure 5, bottom left) shows a significantly different distribution of nitrogen functionalities from that of the HCN polymerization (Figure 1, bottom left). The dipolar sideband pattern for the low-field side of the resonance at 80 ppm (Figure 5, arrow, top left) of the Miller-Urey material is also shown in the figure (top middle). This pattern was obtained by using low-speed magic-angle spinning (for effective dipolar modulation), and a short proton-nitrogen Hartmann-Hahn matched spin-lock contact (so that the spinning sidebands from low-field nonprotonated nitrogen reso-

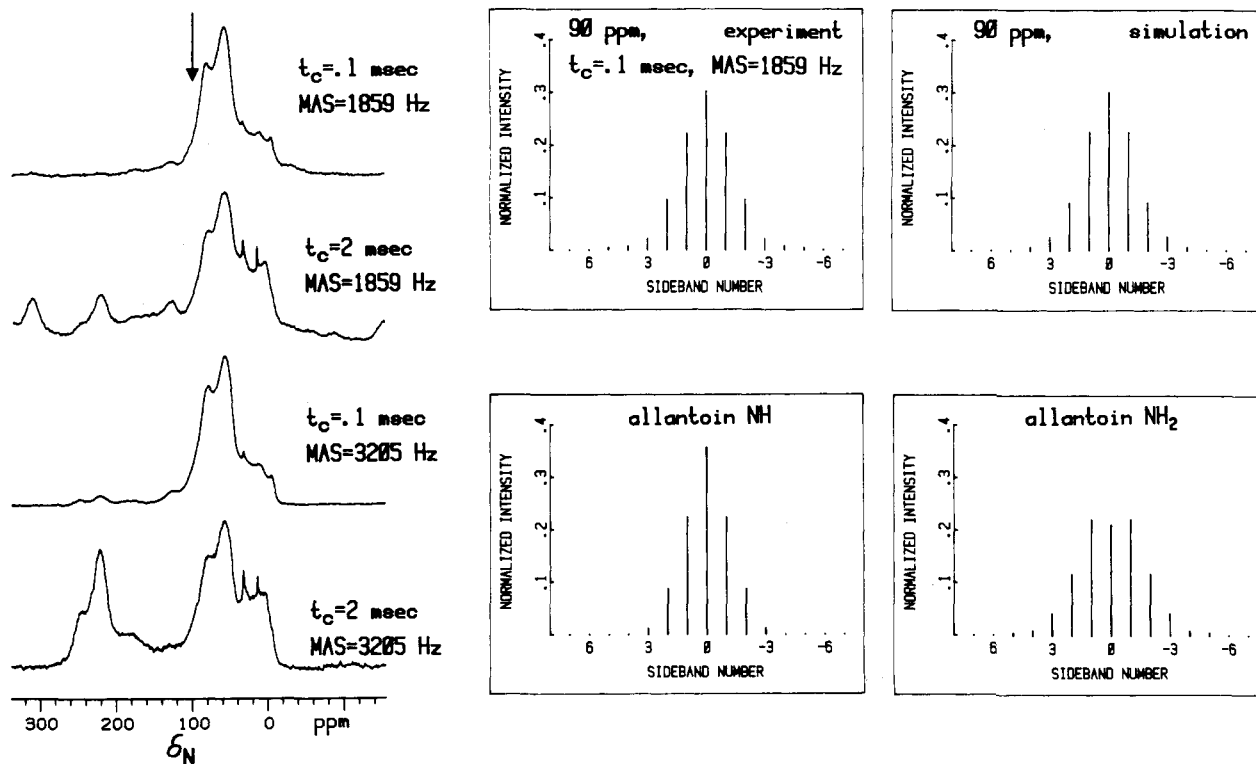


**Figure 5.** 20.3-MHz CPMAS  $^{15}\text{N}$  NMR spectra of the anhydrous solids obtained from electrical discharge through an atmosphere of methane and ammonia (25% enriched in  $^{15}\text{N}$ ). Only the protonated nitrogens have significant intensity with a 0.1-ms proton-nitrogen Hartmann-Hahn matched spin-lock contact (top left). The experimental dipolar rotational sideband pattern (top middle) for the resonance at 90 ppm (arrow, top left) matches that of a simulated pattern produced by adding calculated rigid-lattice NH and  $\text{NH}_2$  patterns in a 66/34 ratio (top right). Experimental NH and  $\text{NH}_2$  patterns for crystalline allantoin are shown at the bottom middle and bottom right, respectively.

**Table I**  
**Dipolar Rotational Sideband Intensities<sup>a</sup> for NH and NH<sub>2</sub> in Some Nitrogen-Containing Solids**

expt or simulation	sideband no.					
	0	1	2	3	4	5
solids from spark discharge						
80 ppm	0.287	0.224	0.102	0.028	0.003	0
90 ppm	0.301	0.221	0.096	0.021	0.007	0.004
water-insoluble solids from base-catalyzed HCN polymer						
80 ppm	0.263	0.221	0.109	0.033	0.006	0.001
90 ppm	0.287	0.220	0.103	0.030	0.004	0.001
95 ppm	0.318	0.221	0.098	0.022	0.002	0.001
allantoin						
NH	0.358	0.224	0.087	0.011	0	0
NH <sub>2</sub>	0.211	0.221	0.117	0.042	0.009	0.005
NH/NH <sub>2</sub> (66/34)	0.309	0.223	0.097	0.021	0.003	0.002
asparagine						
85 ppm	0.221	0.221	0.115	0.044	0.009	0.001
90 ppm	0.214	0.223	0.115	0.044	0.012	0.002
95 ppm	0.207	0.215	0.120	0.047	0.011	0.003
calcd <sup>b</sup>						
NH	0.359	0.227	0.076	0.014	0.003	0
NH <sub>2</sub>	0.188	0.222	0.119	0.049	0.012	0.003
NH/NH <sub>2</sub> (66/34)	0.301	0.225	0.091	0.006	0.001	0

<sup>a</sup>Semiwindowless MREV-8 multiple-pulse decoupling; magic-angle spinning at 1859 Hz. <sup>b</sup>Theoretical rigid-lattice scale factor is 0.54. Effective scale factor<sup>11</sup> is 0.42.

nances were suppressed). The experimental dipolar pattern for the resonance at 90 ppm can be simulated by an average of "rigid-lattice"<sup>11</sup> NH (66%) and NH<sub>2</sub> (34%) dipolar patterns (Figure 5, top right). The simulation used NH and NH<sub>2</sub> calculated rigid-lattice dipolar patterns, but the same result is obtained from a 2 to 1 mix of experimental NH and NH<sub>2</sub> patterns from crystalline allantoin (Table I).

The same combination of NH and NH<sub>2</sub> will also fit the dipolar pattern of the 90-ppm peak of the (HCN)<sub>x</sub> water-treated insolubles (Table I). A significant difference between the two materials is the greater heterogeneity of the resonance of the HCN polymer in this region. Thus, the dipolar pattern of the resonance at 95 ppm for (HCN)<sub>x</sub> (water insolubles) requires about a 75–80% NH contribution, while that at 80 ppm requires less than a 50% contribution (Table I). However, the dipolar patterns at both 80 and 90 ppm in the spectrum of the Miller–Urey material are about the same. The dipolar patterns are also the same for the amide NH<sub>2</sub> of asparagine, regardless of whether the dipolar slice is taken at the 90-ppm center or at each of the half-maximum points of the resonance (Table I).

## Discussion

The absence of significant spectral intensity near 200 ppm in a short-contact experiment (Figure 4, top left) means the Miller–Urey material has little or none of the =NH nitrogen of the amidine functionality. On exposure to water, therefore, this material could not produce heteropolypeptides by reactions I and II. We attribute the observed <sup>15</sup>N 80-ppm peak of the spectrum of the Miller–Urey material to the protonated nitrogens of –NH–CH<sub>2</sub>–N< and –N=C(NH<sub>2</sub>)– groups. Chemical shifts near 80 ppm for the former structure have been observed in urea–melamine polymers<sup>29</sup> and for the latter in vitamin B<sub>1</sub>.<sup>30</sup> The observed dipolar pattern for the resonances in the 80–90 ppm region (Table I) indicates that the –NH–CH<sub>2</sub>–N< groups are present in the greater concentration, and this is consistent with the observation of a strong aliphatic-carbon resonance.

The situation for the base-catalyzed HCN polymer is different. A short contact-time CP transfer experiment showed that this materials has =NH nitrogen (before addition of water), and the spectrum of Figure 1 (bottom

right) shows a reasonably strong resonance at 95 ppm (after the addition of water), the latter also arising from a protonated nitrogen. A protonated nitrogen with this chemical shift is necessarily an amide.<sup>28</sup> The observed dipolar pattern establishes that the amide nitrogen is, for the most part, secondary NH, rather than primary NH<sub>2</sub> (Table I). This conclusion is consistent with the observation of a strong DCP <sup>15</sup>N signal at 95 ppm for the water-treated HCN polymer (Figure 1, top right), attributable to a secondary amide.<sup>10</sup>

Thus, we can conclude that, together with structures like diaminomaleonitrile and the ladder polymers of Völker,<sup>31</sup> the peptide-like structures of eq I are indeed present (at least in low concentrations) in base-catalyzed HCN polymers. But the absence of aliphatic carbons in these materials means the reaction scheme cannot go past eq Ia in the absence of water. In the presence of water, the amidines of eq Ia are apparently converted to the amides of eq II (consistent with the change in intensity at 90–95 ppm in Figure 1, left and right), but the R groups are not the hydrocarbons which would qualify these secondary-amide structures as genuine heteropolypeptides. It is not implausible that minor variations in either the reactants or reaction conditions which we have discussed here will produce both aliphatic carbons and peptide-like nitrogens in the same structure. In fact, preliminary results indicate that aliphatic carbon resonances are observed in the spectra of base-catalyzed HCN polymers, but only following degradative treatment with strong acid. A search for less extreme conditions which produce both aliphatic carbons and peptide-like nitrogens continues.

**Registry No.** HCN (homopolymer), 26746-21-4; allantoin, 97-59-6; asparagine, 70-47-3; ethyl acetamidocyanacetate, 4977-62-2.

## References and Notes

- (1) Matthews, C. N.; Moser, R. E. *Nature (London)* **1967**, *215*, 1230.
- (2) Matthews, C. N.; Moser, R. E. *Proc. Natl. Acad. Sci. U.S.A.* **1966**, *56*, 1087.
- (3) Matthews, C. N. *Origins Life* **1975**, *6*, 155.
- (4) Matthews, C. N. *Origins Life* **1982**, *12*, 281.
- (5) Schopf, J. W., Ed. *Earth's Earliest Biosphere. Its Origins and Evolution*; Princeton University: Princeton, NJ, 1983.
- (6) Matthews, C. N.; Ludicky, R.; Schaefer, J.; Stejskal, E. O.; McKay, R. A. *Origins Life* **1984**, *14*, 243.
- (7) Ferris, J. P. *Science (Washington, D.C.)* **1979**, *203*, 1135.

- (8) Schaefer, J.; McKay, R. A.; Stejskal, E. O. *J. Magn. Reson.* **1979**, *34*, 443.
- (9) Schaefer, J.; Stejskal, E. O.; Garbow, J. R.; McKay, R. A. *J. Magn. Reson.* **1984**, *59*, 150.
- (10) McKay, R. A.; Schaefer, J.; Stejskal, E. O.; Ludicky, R.; Matthews, C. N. *Macromolecules* **1984**, *17*, 1124.
- (11) Schaefer, J.; McKay, R. A.; Stejskal, E. O.; Dixon, W. T. *J. Magn. Reson.* **1983**, *52*, 123.
- (12) Dixon, W. T. *J. Chem. Phys.* **1982**, *77*, 1800.
- (13) Schaefer, J.; Stejskal, E. O. *Top. Carbon-13 NMR Spectrosc.* **1979**, *3*, 384.
- (14) Hester, R. K.; Ackerman, J. L.; Neff, B. L.; Waugh, J. S. *Phys. Rev. Lett.* **1976**, *36*, 1081.
- (15) Stoll, M. E.; Vega, A. J.; Vaughn, R. W. *J. Chem. Phys.* **1976**, *65*, 4093.
- (16) Waugh, J. S.; Huber, L. M.; Haeberlen, U. *Phys. Rev. Lett.* **1968**, *20*, 180.
- (17) Munowitz, M. G.; Griffin, R. G.; Bodenhausen, G.; Huang, T. H. *J. Am. Chem. Soc.* **1981**, *103*, 2529.
- (18) Munowitz, M. G.; Griffin, R. G. *J. Chem. Phys.* **1982**, *76*, 2848.
- (19) Schaefer, J.; Stejskal, E. O.; McKay, R. A.; Dixon, W. T. *Macromolecules* **1984**, *17*, 1479.
- (20) Schaefer, J.; Stejskal, E. O.; Perchak, D.; Skolnick, J.; Yaris, R. *Macromolecules* **1985**, *18*, 368.
- (21) Mansfield, P.; Orchard, M. J.; Stalker, D. C.; Richards, K. H. *B. Phys. Rev.* **1973**, *37*, 90.
- (22) Rhim, W. K.; Elleman, D. D.; Vaughn, R. W. *J. Chem. Phys.* **1973**, *59*, 3740.
- (23) Burum, D. P.; Linder, M.; Ernst, R. R. *J. Magn. Reson.* **1982**, *44*, 173.
- (24) Herzfeld, J.; Berger, A. E. *J. Chem. Phys.* **1980**, *73*, 6021.
- (25) Verbist, J. J.; Lehmann, M. S.; Koetzle, T. F.; Hamilton, W. C. *Acta Crystallogr., Sect. B* **1972**, *B28*, 3006.
- (26) Greenfield, M. S.; Vold, R. L.; Vold, R. R. *J. Chem. Phys.* **1985**, *83*, 1440.
- (27) Fuks, R. *Tetrahedron* **1973**, *29*, 2147.
- (28) See, for example: Witanowski, M.; Stefaniak, L.; Webb, G. A. In *Annual Reports in NMR Spectroscopy*; Webb, G. A., Ed.; Academic: New York, 1981; Vol. IIB.
- (29) Ebdon, J. R.; Heaton, P. E.; Huckerby, T. N.; O'Rourke, W. T. S.; Parkin, J. *Polymer* **1984**, *25*, 821.
- (30) Cain, A. H.; Sullivan, G. R.; Roberts, J. D. *J. Am. Chem. Soc.* **1977**, *99*, 6423.
- (31) Völker, T. *Angew. Chem.* **1960**, *72*, 379.

## Structure of Iodide Ions in Iodinated Nylon 6 and the Evolution of Hydrogen Bonds between Parallel Chains in Nylon 6

N. S. Murthy

*Corporate Technology, Allied-Signal Inc., Morristown, New Jersey 07960.*

*Received April 2, 1986*

**ABSTRACT:** Iodine is present as  $I_5^-$  and  $I_3^-$  ions in iodine-nylon 6 complexes obtained by immersing nylon 6 in an aqueous solution of  $KI/I_2$ . Low-angle X-ray scattering data indicate that in fresh samples the concentration of potassium or iodide ions, or both, is higher in the crystalline lamellar regions than in the interlamellar amorphous regions. It is possible that in some instances iodide ions form sheets and are intercalated between sheets of nylon 6 chains to form a paracrystalline lattice. Two types of  $I_5^-$  columns are identified: in the less stable form the average iodine-iodine distance is 3.2 Å; in the more stable form this distance is 3.08 Å. The  $I_5^-$  ions columns (probably  $H^+I_5^-$ ) interact strongly with nylon 6 molecules and are oriented along the chain axis. The  $I_3^-$  ions (probably  $K^+I_3^-$ ) are weakly bound to nylon 6 and are oriented normal to the chain axis. These intrinsic relations between the iodide ion columns and the nylon chains and the unidirectional diffusion of iodide ions from the surface to the interior of a film causes oriented crystallization of unoriented mobile amorphous regions. This results in the preferential orientation of the crystalline regions in unoriented precursor films immediately after iodination, so that the polymer chains are normal to the surface of the film. Wide-angle X-ray diffraction results suggest that the commensurate structure of  $I_5^-$  columns (average iodine-iodine distance of 3.2 Å) with the nylon 6 chains results in a 15.8–16.0 Å repeat in nylon 6, the shortest observed thus far, which twists the H-bonds out of the plane of the H-bonded sheet. During desorption of the iodine, H-bonds are now readily formed between parallel chains, the chain repeat increases to 16.7–16.9 Å, and the amide groups in the adjacent H-bonded sheets align in one plane. This is usually designated the  $\gamma$  form of nylon 6.

### Introduction

Iodine complexes of polymers are important for many reasons. For example, poly(vinylpyridine)-iodine complexes<sup>1</sup> and nylon 6-iodine complexes<sup>2</sup> can be used as electrode materials in lithium-iodide batteries. Some iodine complexes such as polyacetylene-iodine are also good electrical conductors.<sup>3</sup> When KI is used as a heat stabilizer in engineered parts made from nylon 6, it is quite possible that the iodide ions play an active role. Iodine has two additional effects in nylon 6: it transforms the amorphous or the  $\alpha$  form of nylon 6 into the  $\gamma$  form<sup>4</sup> (in the  $\alpha$  form<sup>5</sup> the hydrogen bonds are formed between fully extended antiparallel chains producing a chain repeat of 17.2 Å; in the  $\gamma$  form<sup>4</sup> these hydrogen bonds are between parallel chains, resulting in a shorter chain repeat of 16.9 Å), and the diffusion of iodine into unoriented films causes the polymer chains to orient normal to the surface of the film.<sup>6,7</sup> To understand the effects of iodine in polymers in general, we studied the most readily available complex,

i.e., iodine-nylon 6. Here we report on the structure of iodide ions and nylon 6 molecules in the complex. We discuss the diffusion-induced oriented crystallization and the resulting orientation of the polymer chains. Finally, we follow the changes in the iodide ion arrays and the changes in the conformation of the nylon 6 chains during iodine desorption.

### Materials and Methods

Commercially available nylon films made by Allied Corp. were used in most of our experiments (intrinsic viscosity 1.34 dL/g;  $M_n \approx 19000$ ;  $M_w \approx 38000$ ; sodium stearate <0.1%; oligomers (up to  $n = 6$ ) including caprolactam <1%; crystallinity of the rolled film  $\sim 15\%$  (mixture of  $\alpha$  and  $\gamma$ ); crystallinity of the drawn (1:3) film  $\sim 50\%$  (mostly  $\alpha$ ); crystallite size in the drawn film  $\sim 45$  Å). Uniaxial orientation was obtained by stretching these films by 1:3 at room temperature. The films were iodinated by immersing the films in an aqueous solution of 1.23 M potassium iodide and 1.23 M iodine for periods ranging from 5 min to 16 h. The term freshly prepared sample is used to designate these iodinated films